metals

MDPI

Article

Study on Preparation of Nano-ZnO by Zinc Hypoxide in Rotary Hearth Furnace

Zhongxue Wang [1], Yun He [2], Weian Wang [2], Yongkun Yang [2], Guoxing Qiu [2] and Xiaoming Li [2,*]

[1] Yinshan Section Steel Corporation of Laiwu Steel Group Ltd., Jinan 271104, China
[2] School of Metallurgical Engineering, Xi'an University of Architecture and Technology, Xi'an 710055, China
* Correspondence: xmli@xauat.edu.cn

Abstract: To realize the high value-added utilization of zinc hypoxide in a rotary hearth furnace, nano-ZnO was prepared by H_2SO_4 wet leaching combined with the Na_2CO_3 precipitation process. The effects of different process conditions on the leaching rate of Zn were analyzed, and the feasibility of preparing nano-ZnO from zinc hypoxide was discussed. The results showed that the optimal process conditions for H_2SO_4 leaching of zinc hypoxide in a rotary hearth furnace were as follows: H_2SO_4 concentration 2.0 mol·L^{-1}, leaching temperature 60 °C, leaching time 90 min, and liquid-solid ratio 8:1. Under these conditions, the leaching rate of Zn reached 95%. The calculation results of leaching kinetics showed that the restrictive link of the H_2SO_4 leaching process was a chemical reaction process; the apparent activation energy was 14.45 kJ·mol^{-1}; and the reaction order was 0.6. The precursor obtained by Na_2CO_3 precipitation treatment was $Zn_5(OH)_6(CO_3)_2$. After calcination at 400 °C, the nano-ZnO with a diameter of less than 100 nm and length greater than 1 μm was obtained. H_2SO_4 leaching combined with the Na_2CO_3 precipitation process provided a new approach for high value-added utilization of zinc hypoxide in a rotary hearth furnace.

Keywords: zinc hypoxide; rotary hearth furnace; Zn leaching rate; leaching kinetics; nano-ZnO

Citation: Wang, Z.; He, Y.; Wang, W.; Yang, Y.; Qiu, G.; Li, X. Study on Preparation of Nano-ZnO by Zinc Hypoxide in Rotary Hearth Furnace. *Metals* **2022**, *12*, 1364. https://doi.org/10.3390/met12081364

Academic Editor: Jean François Blais

Received: 5 July 2022
Accepted: 14 August 2022
Published: 17 August 2022

1. Introduction

Iron and steel production processes inevitably produce the solid waste of dust [1]. With the increase in zinc plating waste steel in steelmaking process, the dust contains a certain amount of valuable metal element zinc [2–6]. Therefore, the recycling of zinc in dust can not only solve the environmental pollution caused by heavy metals, but also produce considerable economic benefits.

The rotary hearth furnace process has gradually become the main method for iron and steel enterprises to deal with metallurgical dust due to its advantages of a large processing capacity, various types of dust, a high dezincification rate and good recovery efficiency [7–10]. In the dust treatment process of a rotary hearth furnace, the zinc oxide in the dust is reduced to elemental zinc at a high temperature and volatilized into the flue gas. The flue gas is cooled to obtain zinc hypoxide [8]. Due to the high content (40–60%) of zinc in zinc hypoxide and the presence by ZnO, it can be easily leached into the solution [11–14]. Liang and Ju et al. found the recovery rate of zinc in rotary hearth furnace dust can reach more than 95% using the wet leaching process [8,15]. Therefore, zinc hypoxide can be used as a raw material for the preparation of zinc-based chemical products to achieve a high value [16].

There are many reports on the preparation of high value-added zinc-based chemical products by zinc-rich dust, but the preparation of basic zinc carbonate or nano-ZnO is mainly based on the waste zinc ash from zinc smelter [17], zinc hypoxide produced by lead-zinc plant [18] or zinc ash produced by a lead fuming furnace [19]. Zhan et al. chose zinc oxide dust as a material and prepared an irregular sheet structure and double cone-shaped nano ZnO under low temperature and alkaline conditions [20]. Darezereshki et al. prepared granular and flake nano ZnO with an electric furnace dust by applying the acid

leaching NH_4OH precipitation method [21]. Yu et al. prepared rod-shaped nano ZnO from electric furnace dust by performing hydrothermal synthesis [22]. Zheng obtained spherical nano ZnO by implementing the wet leaching-$(NH_4)_2CO_3$ precipitation method from zinc tailings [23]. However, there are few studies on acid leaching kinetics and the preparation of nano-ZnO by zinc hypoxide in a rotary hearth furnace. In this paper, the zinc hypoxide in a rotary hearth furnace treated by a domestic iron and steel enterprise was taken as the research object, and nano-ZnO was prepared by H_2SO_4 leaching combined with Na_2CO_3 precipitation. To provide new ideas for the high value-added utilization of zinc hypoxide in a rotary hearth furnace, the effects of different H_2SO_4 leaching processes on the zinc leaching rate were analyzed, and the feasibility of preparing nano-ZnO by Na_2CO_3 precipitation after purification was explored.

2. Experimental Materials and Methods

2.1. Raw Materials

The zinc hypoxide used in the experiment was taken from one certain steel mill in China. The main chemical compositions are shown in Table 1, in which zinc content is 55.15%. The XRD patterns of zinc hypoxide in a rotary hearth furnace is shown in Figure 1. Zinc mainly exists in the form of ZnO, and a small amount exists in the form of $ZnFe_2O_4$.

Table 1. Chemical compositions of zinc hypoxide in rotary hearth furnace (mass fraction, %).

Zn	Pb	Fe	Cu	Cd	Si	Mn	S
55.15	6.75	4.53	0.008	0.07	0.25	0.02	2.46

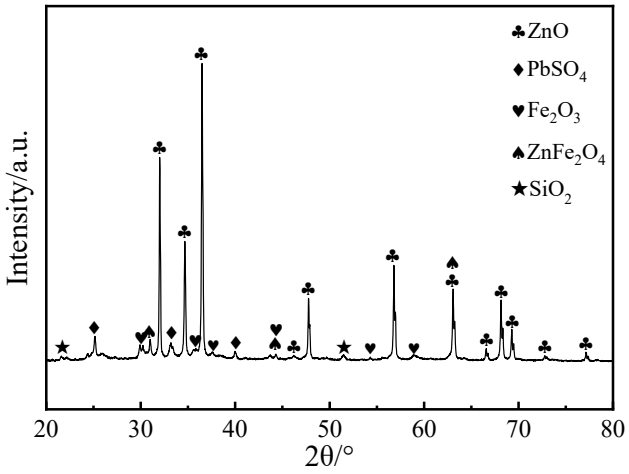

Figure 1. XRD patterns of zinc hypoxide in rotary hearth furnace.

2.2. Experimental Method

(a) Zinc hypoxide leaching experiment

First, the zinc hypoxide was placed in a three-port flask, sulfuric acid was added and then it was placed in a constant temperature water bath at a preset temperature and mechanically stirred using a booster stirrer. After a period of leaching, the liquid–solid separation of the leaching mixture was carried out with a Brinell funnel, and the filter cake was washed 2~3 times. The leaching experiment scheme is shown in Table 2. The concentration of Zn ions in the experimental leaching solution was detected with an atomic absorption spectrophotometer (AA-6800). The zinc leaching rate in zinc hypoxide can be calculated by Equation (1).

$$\eta = \frac{cV}{m\omega} \times 100\% \quad (1)$$

where c is the concentration of the zinc ion in the leaching solution ($g \cdot L^{-1}$), V is the volume of the leaching solution (L), m is the dust sample quality (g), and ω is the mass fraction of zinc element (%).

Table 2. Experimental Scheme of Zinc Oxide Leaching.

	Concentration of Sulphuric Acid/mol·L^{-1}	Leaching Temperature/°C	Liquid-Solid Ratio	Leaching Time/min
concentration of sulphuric acid	0.5, 1.0, 2.0, 2.5, 3.0	60	10:1	90
leaching temperature	2.0	30, 40, 50, 60, 70, 80	10:1	90
liquid-solid ratio	2.0	60	5:1, 6:1, 7:1, 8:1, 9:1, 10:1	90
leaching time	2.0	60	8:1	30, 60, 90, 120, 150, 180

(b) Precipitation experiment of nano-ZnO

Before the precipitation experiment of the leaching solution, the leaching solution was purified. Firstly, Fe was removed by implementing the goethite-oxidation hydrolysis method. Secondly, Fe and Mn were thoroughly removed using ammonium persulfate. Finally, Cd, Cu and other impurities were removed using the zinc powder replacement method to obtain a high-purity $ZnSO_4$ solution. After purification, the concentration of each element in the leaching solution is shown in Table 3. The impurity element content in the leaching solution is very low, which can be directly used to prepare nano-ZnO.

Table 3. Contents of elements after purification ($g \cdot L^{-1}$).

Zn	Pb	Fe	Cu	Cd	Si	Mn
27.91	—	<0.0001	<0.0001	<0.0001	—	—

At room temperature, the purified leaching solution (Zn^{2+} concentration of 0.5 $mol \cdot L^{-1}$) was added to the continuously stirred Na_2CO_3 solution (concentration of 1.0 $mol \cdot L^{-1}$) according to the equal volume ratio. After the addition, the solution was stirred for 30 min. Then, the solution was filtered and washed with deionized water and ethanol many times. The precipitate was dried at 90 °C for 4 h in a blast dryer to obtain nano-ZnO precursor. The obtained precursor was grinded into fine powder particles and calcined at 400 °C for 30 min in a muffle furnace to obtain the final product nano-ZnO. An X-ray diffractometer (XRD, D8 ADVANCE A25, Bruker, Billerica, MA, USA) and scanning electron microscope (SEM, Gemini SEM 300, Zeiss, Oberkochen, Germany) were used to analyze the phase and morphology of nano-ZnO.

3. Kinetic Model of Leaching Zinc Hypoxide

The wet leaching process is a solid–liquid multiphase reaction, and this process has multiple stages such as adsorption, diffusion and chemical reaction [24,25]. Zinc in zinc-rich dust mainly exists in the form of ZnO, and the leaching reaction is a typical liquid–solid reaction. The leaching process is a heterogeneous reaction between solid particles and the liquid phase. The shrinking unreacted core model is the best model to reflect the actual situation of the leaching process, as shown in Figure 2. The leaching process is mainly composed of the following steps [26]:

(1) H^+ in the solution diffuses from the solution to the surface of solid particles;
(2) H^+ diffuses through the product layer film to the surface of the unreacted core;
(3) Reaction on the surface of the unreacted nucleus;
(4) Reaction products diffuse from the reaction interface to the surface of solid particles through solid film;
(5) Reaction product diffuses from the reaction interface to the surface of the product layer.

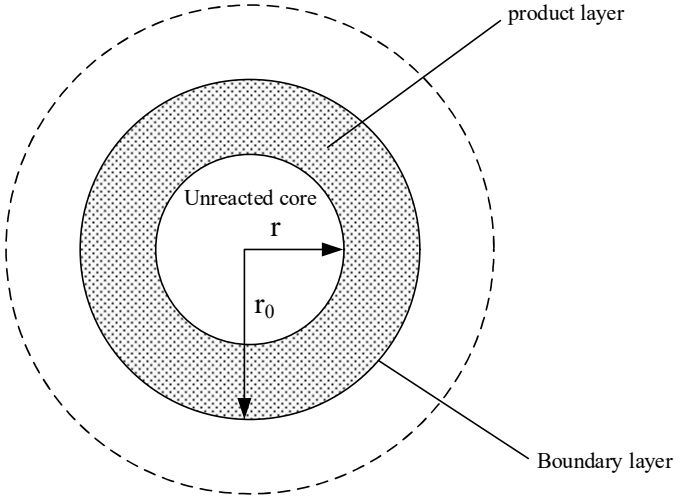

Figure 2. The shrinking unreacted core model of spherical solid particles.

If the leaching reaction is controlled by means of a chemical reaction, the kinetic equation of the leaching process can be expressed by Equation (2). If the leaching reaction is diffusion controlled, the kinetic equation can be expressed by Equation (3).

$$1 - (1 - \alpha)^{1/3} = k \times t \tag{2}$$

$$1 - 2/3 \times \alpha - (1 - \alpha)^{2/3} = k \times t \tag{3}$$

where α is the zinc leaching rate of the reaction time t; k is the apparent reaction rate constant controlled by the chemical reaction.

Based on the dynamic model of diffusion and interfacial mass transfer mixed control, the apparent rate constant k of the leaching process is obtained, and the apparent activation energy of the zinc leaching process is calculated by combining the Arrhenius equation [27], as shown in Equations (4) and (5).

$$\ln k = -\frac{E_\alpha}{R}\left(\frac{1}{T}\right) + \ln A \tag{4}$$

$$E_\alpha = -k_s \times R \tag{5}$$

where k is the apparent rate constant (min^{-1}); A is the pre-exponential factor; T is the reaction temperature (K); R is the ideal gas constant (8.314 J/(mol·K)); E_α is the apparent activation energy of the reaction ($kJ \cdot mol^{-1}$); and k_s is the slope of the linear equation.

4. Results and Discussion

4.1. Effect of Different Factors on Zinc Leaching Rate

(a) Concentration of sulphuric acid

Figure 3 shows the effect of different sulfuric acid concentrations on the zinc leaching rate in zinc hypoxide. With the increase in the sulfuric acid concentration, the zinc leaching rate increases. When the sulfuric acid concentration is 0.5~1.5 $mol \cdot L^{-1}$, the leaching rate increases from 59.39% to 91.41%, showing a rapid upward trend. When the sulfuric acid concentration is 2.0 $mol \cdot L^{-1}$, the leaching rate is 94.93%. When the sulfuric acid concentration increases to 3.0 $mol \cdot L^{-1}$, the leaching rate changes gradually, which indicates that when the concentration of sulfuric acid is 2.0 $mol \cdot L^{-1}$, the dissolution state of zinc ions is close to saturation. With the continuous increase in the sulfuric acid concentration, the leaching rate of zinc increases by only 1.11%. Although increasing the concentration of sulfuric acid will correspondingly increase the concentration of H^+ in the reaction, which is conducive to the leaching of zinc in the sample, as the reaction continues, H^+ in the solution is gradually consumed, and the leaching rate gradually slows down [28]. Therefore,

considering the leaching rate and the cost of Zn, the optimum sulfuric acid concentration is 2.0 mol·L^{-1}.

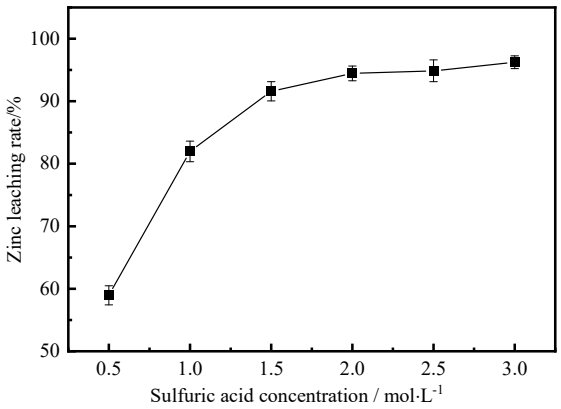

Figure 3. Effect of sulfuric acid concentration on zinc leaching rate.

(b) Leaching temperature

Figure 4 shows the effect of different leaching temperatures on the zinc leaching rate in zinc hypoxide. With the increase in leaching temperature, the leaching rate of zinc increases. When the reaction temperature increases from 30 °C to 60 °C, the zinc leaching rate increases from 88.49% to 94.85%; when the temperature continues to increase to 80 °C, the zinc leaching rate does not change significantly. When the temperature of the reaction system increases, the number of activated molecules increases; the diffusion coefficient of metal ions increases; and the dissolution rate accelerates. The viscosity of the solution decreases with the increase in temperature. The decrease in viscosity can accelerate the diffusion rate of molecules and ions, which accelerates the chemical reaction and accelerates the whole process in general [29]. However, when the temperature is too high, the water evaporation is accelerated as the water bath is heated, which is unfavorable to the reaction. Therefore, the optimal leaching temperature is 60 °C.

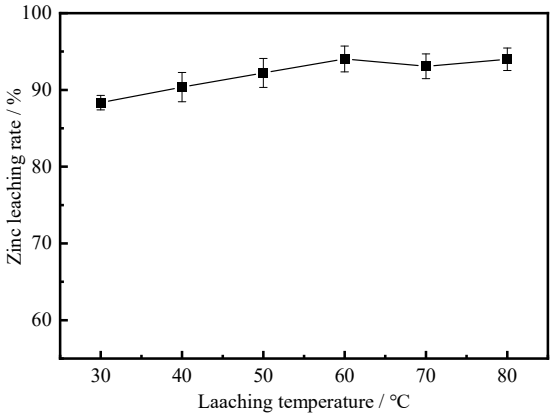

Figure 4. Effect of leaching temperature on zinc leaching rate.

(c) Liquid-solid ratio

Figure 5 shows the effect of liquid-solid ratio on zinc leaching rate in zinc hypoxide. With the increase in the liquid–solid ratio, the zinc leaching rate increases. When the liquid–solid ratio is 5:1, the zinc leaching rate is 77.34%. As the liquid–solid ratio increases to 8:1, the zinc leaching rate reaches 94.65%. The liquid–solid ratio not only affects the consumption of sulfuric acid, but also affects the viscosity of the solution, thereby affecting the leaching rate and subsequent treatment. Increasing the liquid–solid ratio of the leaching reaction can reduce the viscosity of the solution, which is conducive to slurry mixing and

solid–liquid separation [30]. However, when the residual sulfuric acid concentration is the same, the consumption of sulfuric acid increases, and the subsequent waste acid treatment is large. If the liquid–solid ratio is too little, the solution volume is too small and the stirring is difficult, resulting in the settlement of the sample at the bottom. At the beginning of leaching, the liquid–solid ratio increases to maintain greater unsaturation in the leaching process, and the viscosity of the solution is reduced. The reactants and products at the solid–liquid interface are exchanged and diffused, which is conducive to the acid leaching reaction and increases the leaching rate of zinc [31].

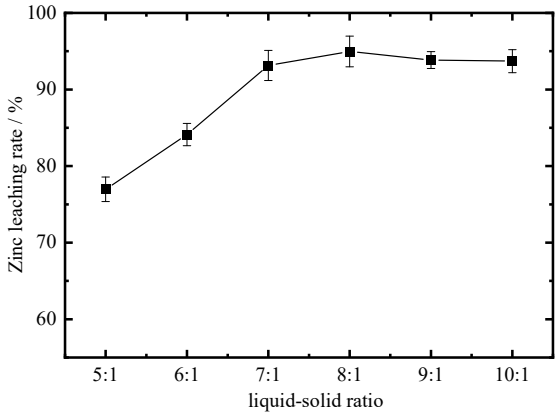

Figure 5. Effect of liquid-solid ratio on zinc leaching rate.

When the liquid–solid ratio increases from 8:1 to 10:1, the leaching rate of zinc is almost unchanged, with a small increase and basically tends to be balanced. This is because with the continuous increase in the liquid–solid ratio, the saturation of the solid–liquid interface does not change, and the zinc leaching rate basically does not increase, which will cause the waste of the acid solution. Therefore, the optimal liquid–solid ratio in the leaching process is 8:1.

(d) Leaching time

Figure 6 shows the effect of different leaching times on the zinc leaching rate in zinc hypoxide. When the leaching time increased from 30 min to 90 min, the zinc leaching rate demonstrated a rapid upward trend. This is because at the beginning of the reaction, a large number of metal ions enter the sulfuric acid solution. When the reaction time is prolonged, the ion concentration in the solution increases, and it takes enough time to react. When the leaching time is within 30 min, zinc hypoxide reacts strongly with sulfuric acid, and 80% of zinc in zinc hypoxide can be leached. With the extension of time, the leaching rate of zinc has a slow upward trend. When the leaching time is 90 min, the leaching rate of zinc reaches the maximum. Furthermore, as the leaching time increases to 120 min, the leaching rate of zinc does not change significantly, but when the leaching time increases to 150 min, the leaching rate of zinc decreases. This may be due to the formation of colloidal substances between iron and other elements, which coat the leached zinc, leaving some zinc in the leaching residue and resulting in the decrease in the zinc leaching rate. Therefore, the optimal leaching time is 90 min.

4.2. Determination of Kinetic Parameters of Zinc OXIDE Leaching

Figure 7 shows the variation in the zinc leaching rate with leaching time under different sulfuric acid concentrations. With the increase in the sulfuric acid concentration, the zinc leaching rate increases, and with the extension of time, the zinc leaching rate tends to be gradual. This is because increasing the concentration of sulfuric acid increases the concentration of H^+ in the leaching system accordingly. A high concentration of H^+ is beneficial for zinc ions to enter the solution. However, with increasing time, H^+ in the solution is gradually consumed, and the leaching rate gradually slows down. The data in

Figure 7 are fitted and analyzed, and the leaching kinetics curve is obtained according to Equation (2), as shown in Figure 8.

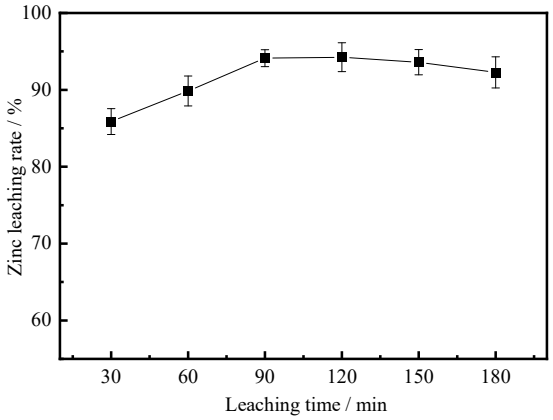

Figure 6. Effect of leaching time on zinc leaching rate.

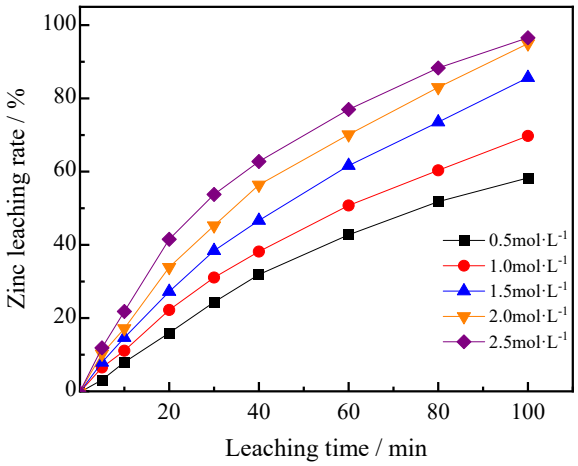

Figure 7. Variation of Zinc leaching rate with leaching time under different sulfuric acid concentrations.

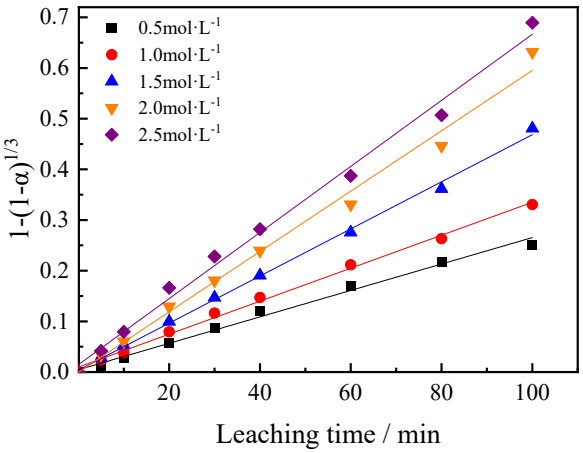

Figure 8. Leaching kinetics curves under different sulfuric acid concentrations.

Linear fitting is performed on each curve in Figure 8, and the slope of the obtained straight line is the reaction rate constant k. The slope k of the straight line increases with the increase in the sulfuric acid concentration, indicating that the zinc leaching rate is accelerated. The relationship between ln k and ln[H_2SO_4] was investigated. The fitting curve in Figure 9 shows that the reaction order of leaching zinc is 0.6.

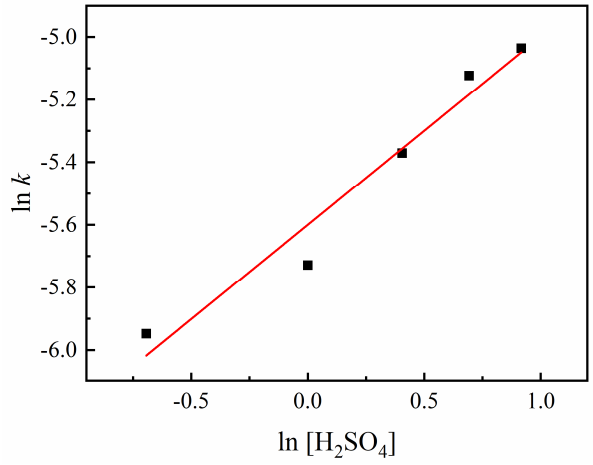

Figure 9. Relationship between ln k and ln[H_2SO_4].

Figure 10 shows the variation in the zinc leaching rate with leaching time at different leaching temperatures. With the increase in the leaching temperature, the leaching rate of zinc increases continuously. However, with the extension of leaching time, the curve of the zinc leaching rate gradually tends to be flat, and the growth trend becomes slow. The data in Figure 10 are fitted, and the leaching kinetics curve is obtained according to Equation (2). Figure 11 shows that the linear slope k increases with the increase in the leaching temperature, indicating that the leaching rate of zinc is accelerated.

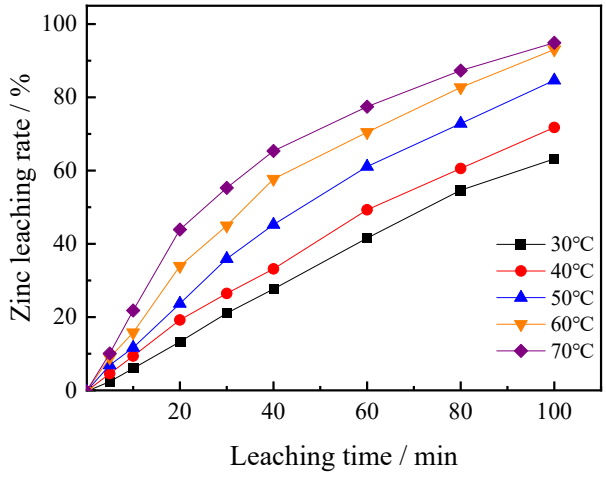

Figure 10. Curves of zinc leaching rate changing with time at different temperatures.

According to the k value obtained in Figure 11, the scatter plot of the relationship between ln k and $1/T$ is plotted, and the linear fitting was performed. The results are shown in Figure 12. The apparent activation energy of zinc leaching calculated by Equation (5) is 14.45 kJ/mol, which proves that the controlling step of zinc leaching is the chemical reaction process.

4.3. Characteristics of Nano-ZnO

The phase of the prepared nano-ZnO precursor is detected by XRD, and the XRD diffraction pattern is shown in Figure 13. The diffraction peaks of 2θ values at 12.96°, 28.18°, 31.25°, 33.12°, 36.13° and 59.57° correspond to the crystal plane of the monoclinic $Zn_5(OH)_6(CO_3)_2$ crystal, which indicates that the precursor is composed of pure monoclinic $Zn_5(OH)_6(CO_3)_2$. Figure 14 is the SEM image of the nano-ZnO precursor. Nano-ZnO precursor presents aggregated flakes and fluffy textures, and the surface shows roughness and certain gaps exist.

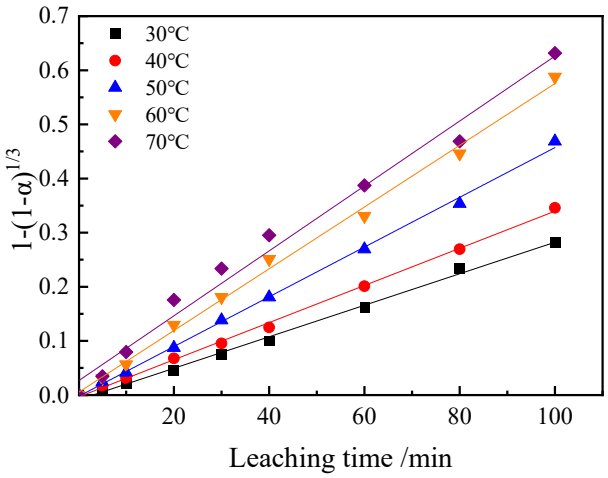

Figure 11. Leaching kinetics curves under different leaching time.

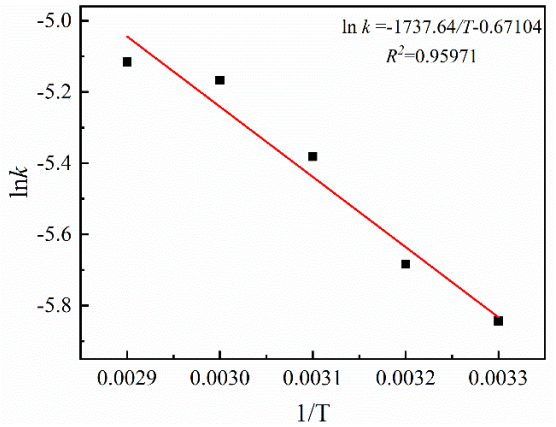

Figure 12. Relationship between ln k and $1/T$.

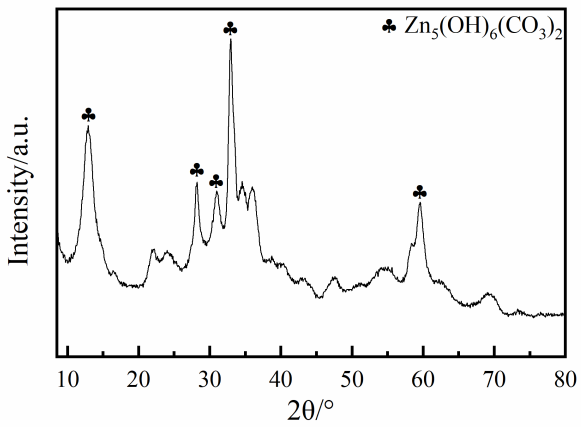

Figure 13. XRD patterns of nano-ZnO precursors.

The phase and crystallization degree of nano-ZnO were analyzed by performing XRD, which confirmed that nano-ZnO particles have single-phase and polycrystalline properties. The analysis results are shown in Figure 15. The 2θ values at 31.77°, 34.35°, 35.86°, 47.25°, 56.50°, 62.53°, 66.18°, 67.69°, 68.76° and 76.50° correspond to (100), (002), (101), (102), (110), (103), (200), (112), (201) and (202) crystal planes, respectively. These are consistent with the JCPDS standard card of zinc oxide (PDF # 36-1451), indicating that the nanostructure of zinc oxide is related to the wurtzite structure of high purity zinc oxide. In addition, the diffraction peak is sharp. Meanwhile, no diffraction peaks corresponding to metal zinc or any other form of zinc compound are observed in Figure 15, indicating that the precipitate

is a single crystalline zinc oxide with good crystallinity [32,33]. In addition, it can be seen from Figure 15 that (100), (002) and (101) crystal planes have high-intensity diffraction peaks, and the diffraction from multiple planes indicates the random orientation of the synthesized nanostructure. The diffraction peak with the highest intensity is a (101) crystal plane rather than a (002) crystal plane, indicating that the preferential growth along the c-axis in the hexagonal structure is hindered.

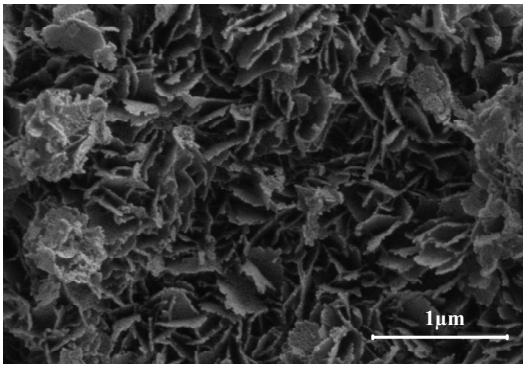

Figure 14. SEM morphologies of nano-ZnO precursor.

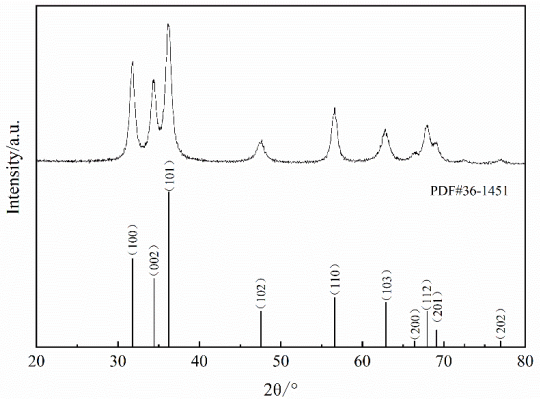

Figure 15. XRD patterns of nano-ZnO.

The morphologies of nano-ZnO are shown in Figure 16. The experimental precipitation product is a linear nanometer zinc oxide with close arrangement and high density. The diameter of the product nanowires is less than 100 nm, and the length is greater than 1 μm. In addition, due to the lack of morphological control, the precipitation products have agglomeration phenomenon. Combined with the phase analysis of the nano-ZnO precursor in Figure 15, the product is a hexagonal wurtzite structure. The nano-ZnO prepared by this process has good crystallinity and high purity.

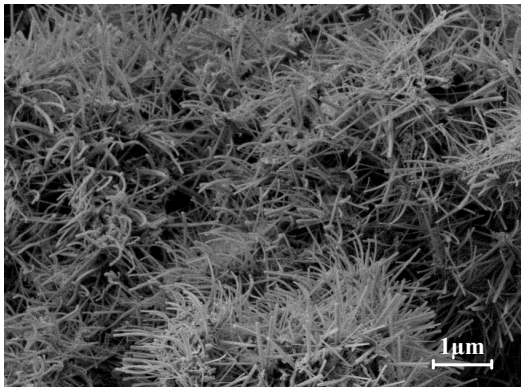

Figure 16. SEM morphologies of nano-ZnO.

5. Conclusions

In this paper, the zinc hypoxide from a rotary hearth furnace was taken as the research object. The effects of different process conditions on the leaching rate of Zn were studied by performing H_2SO_4 wet leaching, and the process feasibility of preparing high value-added nano-zinc oxide from zinc hypoxide was discussed. The results are as follows:

(1) The optimum process conditions for H_2SO_4 treatment of zinc oxide in a rotary hearth furnace are as follows: leaching agent concentration of 2.0 mol·L^{-1}, leaching temperature of 60 °C, leaching time of 90 min, liquid-solid ratio of 8:1, and zinc leaching rate of 95%.

(2) The kinetic calculation results show that the restrictive link of the H_2SO_4 leaching process is chemical reaction control, the apparent activation energy is 14.45 kJ·mol^{-1}, and the reaction order is 0.6.

(3) The nano-ZnO precursor is $Zn_5(OH)_6(CO_3)_2$. After calcination at 400 °C, the precursor is completely decomposed to nano-ZnO. The morphology of nano-ZnO is nanowires with high crystallinity. The diameter of nanowires is less than 100 nm and the length of nanowires is greater than 1 μm. It is feasible to prepare high value-added nano-ZnO by performing H_2SO_4 leaching combined with the Na_2CO_3 precipitation process with zinc hypoxide as the raw material.

Author Contributions: Conceptualization, X.L., Z.W. and Y.Y.; Methodology, X.L., Z.W and G.Q.; Software, W.W. and Y.H.; Validation, Z.W. and X.L.; Formal analysis, X.L. and Y.H.; Investigation, X.L. and W.W.; Resources, Z.W., G.Q. and Y.Y.; Data curation, X.L. and Z.W.; Writing—original draft preparation, X.L. and Z.W.; Writing—review and editing, X.L. and Z.W.; Visualization, Z.W.; Supervision, W.W.; Project administration, G.Q.; Funding acquisition, Y.Y. All authors have read and agreed to the published version of the manuscript.

Funding: This research was supported by the National Natural Science Foundation of China (No. 51774224) and the Natural Science Basic Research Plan in Shaanxi Province of China (No. 2019JLM-35).

Institutional Review Board Statement: Not applicable.

Informed Consent Statement: Not applicable.

Data Availability Statement: Not applicable.

Conflicts of Interest: The authors declare no conflict of interest.

References

1. Vestola, E.A.; Kuusenaho, M.K.; Närhi, H.M. Acid bioleaching of solid waste materials from copper, steel and recycling industries. *Hydrometallurgy* **2010**, *103*, 74–79. [CrossRef]
2. Hou, S.; Zheng, N.; Tang, L. Pollution characteristics, sources, and health risk assessment of human exposure to Cu, Zn, Cd and Pb pollution in urban street dust across China between 2009 and 2018. *Environ. Int.* **2019**, *128*, 430–437. [CrossRef] [PubMed]
3. Chirenje, T.; Ma, L.Q.; Lu, L. Retention of Cd, Cu, Pb and Zn by wood ash, lime and fume dust. *Water Air Soil Pollut.* **2006**, *171*, 301–314. [CrossRef]
4. Sofilić, T.; Rastovčan-Mioč, A.; Cerjan-Stefanović, Š. Characterization of steel mill electric-arc furnace dust. *J. Hazard. Mater.* **2004**, *109*, 59–70. [CrossRef]
5. Laforest, G.; Duchesne, J. Characterization and leachability of electric arc furnace dust made from remelting of stainless steel. *J. Hazard. Mater.* **2006**, *135*, 156–164. [CrossRef]
6. Nyirenda, R.L. The processing of steelmaking flue-dust: A review. *Miner. Eng.* **1991**, *4*, 1003–1025. [CrossRef]
7. Oda, H.; Ibaraki, T.; Abe, Y. Dust recycling system by the rotary hearth furnace. *Shinnittetsu Giho* **2006**, *384*, 134.
8. Ju, D.; Yao, H.; Ma, H. Removal process and mechanism of lead in Zn-containing rotary hearth furnace dust. *Inorg. Chem. Commun.* **2021**, *127*, 108496. [CrossRef]
9. Wang, J.; Zhang, Y.; Cui, K. Pyrometallurgical recovery of zinc and valuable metals from electric arc furnace dust–a review. *J. Clean Pract.* **2021**, *298*, 126788. [CrossRef]
10. Wu, Y.; Jiang, Z.; Zhang, X. Numerical simulation of the direct reduction of pellets in a rotary hearth furnace for zinc-containing metallurgical dust treatment. *Int. J. Min. Met. Mater.* **2013**, *20*, 636–644. [CrossRef]
11. Li, H.; Zhao, L.; Wang, L. Leaching Kinetics of Zinc hypoxide in a NH_3–NH_4HCO_3–H_2O System. *Crystals* **2021**, *11*, 496. [CrossRef]
12. Jiang, T.; Zhang, T.; Ye, F. Occurrence state and sulfuric-acid leaching behavior of germanium in zinc hypoxide. *Miner. Eng.* **2019**, *137*, 334–343. [CrossRef]

13. Lottering, C. *Leaching of Zinc Hypoxides Using Sulphuric Acid*; Stellenbosch University: Stellenbosch, South Africa, 2016.
14. Jiang, T.; Meng, F.; Gao, W. Leaching behavior of zinc from crude zinc oxide dust in ammonia leaching. *J. Cent. South Univ.* **2021**, *28*, 2711–2723. [CrossRef]
15. Liang, S.; Liang, X.; Tang, Q. Treatment of Secondary Dust Produced in Rotary Hearth Furnace through Alkali Leaching and Evaporation–Crystallization Processes. *Processes* **2020**, *8*, 396. [CrossRef]
16. Luptáková, N.; Pešlová, F.; Kliber, J. The study and microstructure analysis of zinc and zinc oxide. *Metalurgija* **2015**, *54*, 43–46.
17. Yang, C.S.; Ren, M.X. Practice of waste dust mud treatment in Rizhao Steel. *J. Iron Steel Res. Int.* **2019**, *54*, 83–91+98.
18. Wang, H.J.; Kang, W.T.; Ma, L. New process for the preparation of active zine oxide from zinc. *Inorg. Chem. Ind.* **2006**, *38*, 55–56.
19. Kang, W.G.; Wang, W.; Wang, J.C. Process research on production of sub-zinc oxide in lead-smoke furnace. *China Resour. Compr. Util.* **2019**, *37*, 173–177.
20. Zhan, F.; Yang, L.J.; Guo, X.W. Growth mechanism of double cone-shaped nano zinc oxide prepared from zinc oxidation flue dusts by acid leaching. *Ferroelectrics* **2022**, *593*, 26–36. [CrossRef]
21. Darezereshki, E.; Vakylabad, A.B.; Koohestani, B. A Hydrometallurgical Approach to Produce Nano-ZnO from Electrical Arc Furnace Dusts. *Min. Metall. Explor.* **2021**, *38*, 1525–1535. [CrossRef]
22. Yu, B.S.; Wang, Y.R.; Chang, T.C. Hydrothermal treatment of electric arc furnace dust. *J. Hazard. Mater.* **2011**, *190*, 397–402. [CrossRef] [PubMed]
23. Zhen, Y.S. *Study on Preparation of Nanometer Zinc Oxide from Zinc Tail of a Silver Ore [D]*; Wuhan Institute of Technology: Wuhan, China, 2020.
24. Zhang, W.C.; Noble, A.; Yang, X.B.; Honaker, R. Lithium leaching recovery and mechanisms from density fractions of an Illinois Basin bituminous coal. *Fuel* **2020**, *268*, 117319. [CrossRef]
25. Dickinson, C.F.; Heal, G.R. Solid–liquid diffusion controlled rate equations. *Thermochim. Acta* **1999**, *340–341*, 89–103. [CrossRef]
26. Idachaba, M.A.; Nyavor, K.; Egiebor, N.O. Kinetic analysis of data obtained from studies on microbial degradation of cement waste forms, using shrinking core models. *J. Hazard. Mater.* **2003**, *99*, 57–69. [CrossRef]
27. Kim, C.; Yoon, H.; Chung, K.W.; Lee, J.Y.; Kim, S.D. Leaching kinetics of lanthanum in sulfuric acid from rare earth element (REE) slag. *Hydrometallurgy* **2014**, *146*, 133–137. [CrossRef]
28. Zhang, J.X.; Zou, X.; Niu, F.S. Leaching behavior and leaching kinetics of zinc from zinc-bearing dust. *Chin. J. Nonferr. Met.* **2018**, *28*, 1688–1696.
29. Li, J.; Li, C.Y.; Li, B.W. Acid leaching of low grade rare earth concentrate by microwave heating. *Chin. J. Rare Met.* **2014**, *38*, 839–845.
30. Yan, W.B.; Hu, L.S.; Gao, F. Effect of manganese dioxide on acid leaching of vanadium from stone coal. *Chin. J. Rare Met.* **2013**, *37*, 130–134.
31. Xie, W.M.; Zhang, N.; Li, J. Optimization of condition for extraction of aluminum and iron from red mud by hydrochloric acid leaching. *J. Environ. Eng.* **2017**, *11*, 5677–5682.
32. Wang, Q. *Study on Doping Characteristics of Nanostructured ZnO [D]*; Yantai University: Yantai, China, 2018.
33. Wu, L.Z.; Qi, D.; Yin, Y.L. Study on the synthesis of nanometer zinc oxide. *Yunnan Chem. Technol.* **2018**, *45*, 12–14.